Published for SISSA by Springer

Received: *September 4, 2024*
Revised: *September 27, 2024*
Accepted: *October 14, 2024*
Published: *November 8, 2024*

Measurement of Born cross sections of $e^+e^- \to \Xi^0\bar{\Xi}^0$ and search for charmonium(-like) states at $\sqrt{s} = 3.51$–$4.95\,\text{GeV}$

The BESIII collaboration

E-mail: besiii-publications@ihep.ac.cn

Abstract: Using e^+e^- collision data collected by the BESIII detector at BEPCII corresponding to an integrated luminosity of $30\,\text{fb}^{-1}$, we measure Born cross sections and effective form factors for the process $e^+e^- \to \Xi^0\bar{\Xi}^0$ at forty-five center-of-mass energies between 3.51 and 4.95 GeV. The dressed cross section is fitted, assuming a power-law function plus a charmonium(-like) state, i.e., $\psi(3770)$, $\psi(4040)$, $\psi(4160)$, $\psi(4230)$, $\psi(4360)$, $\psi(4415)$ or $\psi(4660)$. No significant charmonium(-like) state decaying into $\Xi^0\bar{\Xi}^0$ is observed. Upper limits at the 90% confidence level on the product of the branching fraction and the electronic partial width are provided for each decay. In addition, ratios of the Born cross sections and the effective form factors for $e^+e^- \to \Xi^0\bar{\Xi}^0$ and $e^+e^- \to \Xi^-\bar{\Xi}^+$ are also presented to test isospin symmetry and the vector meson dominance model.

Keywords: e^+-e^- Experiments, Particle and Resonance Production, QCD

ArXiv ePrint: 2409.00427

https://doi.org/10.1007/JHEP11(2024)062

Contents

1 Introduction 1

2 BESIII detector and Monte Carlo simulation 2

3 Event selection 3

4 Born cross section measurement 4
- 4.1 Determination of signal yields 4
- 4.2 Determination of Born cross section and effective form factor 5

5 Systematic uncertainty 5
- 5.1 Luminosity 5
- 5.2 Ξ^0 reconstruction 8
- 5.3 Background 8
- 5.4 Angular distribution 8
- 5.5 Branching fractions 8
- 5.6 Input line shape 8
- 5.7 Total systematic uncertainty 8

6 Fit to the dressed cross section 9

7 Summary 9

The BESIII collaboration 18

JHEP11(2024)062

1 Introduction

In 1974, the first member of charmonium family, the J/ψ particle, was discovered [1, 2]. It provided support for the existence of a fourth quark, called the charmed quark. A series of charmonium states have been observed at e^+e^- colliders in the past decades. Three conventional charmonium states, i.e., $\psi(4040)$, $\psi(4160)$, and $\psi(4415)$ [3], observed in the inclusive hadronic cross section and dominated by open-charm final states, agree well with the predictions of the potential model [4]. Another five charmonium-like states, i.e. $\psi(4230)$, $\psi(4260)$, $\psi(4360)$, $\psi(4634)$, and $\psi(4660)$, were observed via the initial state radiation (ISR) process by the Belle and BaBar experiments [5–13], and via direct production processes by the CLEO [14] and BESIII experiments [15, 16]. The unexpected multitude of states and mismatch of quantum numbers predicted by the potential model have given rise to a great deal of interest. Various hypotheses have been proposed to explain their nature [17–24], including hybrid states, multiple-quark states, and molecular structures. However, up to now, no definitive conclusion has been drawn.

This situation indicates an incomplete understanding of the strong interaction, and to help clarify this, more experimental information is needed. In particular, the study of two-body

baryonic decays of charmonium(-like) states, $\psi(3770)$, $\psi(4040)$, $\psi(4160)$, $\psi(4230)$, $\psi(4360)$, $\psi(4415)$ and $\psi(4660)$, and their subsequent hadronic decays in e^+e^- collisions provide a new window for understanding the nature of these states. In addition, the measurement of the electromagnetic form factors or the effective form factor would also provide insight into the internal structure of the charmonium(-like) states. Although many experimental studies [25–34] of baryon anti-baryon ($B\bar{B}$) pair production have been performed above open-charm threshold by the BESIII and Belle experiments, the only evidence for $B\bar{B}$ final states from vector charmonium(-like) decay is for $\psi(3770) \to \Lambda\bar{\Lambda}$ and $\psi(3770) \to \Xi^-\bar{\Xi}^+$ [27, 31]. Thus, more precise measurements of exclusive cross sections for the $e^+e^- \to B\bar{B}$ reactions are needed to further investigate the nature of the charmonium(-like) states above open charm threshold. Further, as proposed by ref. [35], the measured ratios of the Born cross section or the effective form factor between the $e^+e^- \to \Xi^0\bar{\Xi}^0$ process and its isospin partner processes is important to validate the prediction based on the vector meson dominance model [36–40].

In this article, we present measurements of the Born cross sections and the effective form factors for the $e^+e^- \to \Xi^0\bar{\Xi}^0$ reaction, in the range of center-of-mass (CM) energy $\sqrt{s}$ between 3.51 and 4.95 GeV. These measurements are based on e^+e^- collision data with a total integrated luminosity of 30 fb^{-1}, collected by the BESIII detector [41] at BEPCII [42]. Measurements from the CLEO-c experiment [43] are also shown for comparison. Possible resonances are searched for by analyzing the line shape of the dressed cross sections of the $e^+e^- \to \Xi^0\bar{\Xi}^0$ reaction. The product of branching fractions and electronic partial widths for charmonium(-like) states decaying into $\Xi^0\bar{\Xi}^0$ as well as their upper limits at the 90% confidence level (C.L.) are reported. In addition, the ratios of the Born cross section and the effective form factor for the reactions of $e^+e^- \to \Xi^0\bar{\Xi}^0$ and $e^+e^- \to \Xi^-\bar{\Xi}^+$ from the BESIII experiment [31] are presented.

2 BESIII detector and Monte Carlo simulation

The BESIII detector [41] records symmetric e^+e^- collisions provided by the BEPCII storage ring [42] in the range of $\sqrt{s}$ from 1.85 to 4.95 GeV, with a peak luminosity of $1.1\times10^{33}\,\mathrm{cm}^{-2}\,\mathrm{s}^{-1}$ achieved at $\sqrt{s} = 3.773$ GeV. BESIII has collected large data samples in this energy region [44–46]. The cylindrical core of the BESIII detector covers 93% of the full solid angle and consists of a helium-based multilayer drift chamber (MDC), a time-of-flight system (TOF), and a CsI(Tl) electromagnetic calorimeter (EMC), which are all enclosed in a superconducting solenoidal magnet providing a 1.0 T magnetic field. The solenoid is supported by an octagonal flux-return yoke with resistive plate counter muon identification modules interleaved with steel. The charged-particle momentum resolution at 1 GeV/c is 0.5%, and the dE/dx resolution is 6% for electrons from Bhabha scattering. The EMC measures photon energies with a resolution of 2.5% (5%) at 1 GeV in the barrel (end cap) region. The time resolution of the plastic-scintillator TOF system in the barrel region is 68 ps, while that in the end cap region was 110 ps. The end cap TOF system was upgraded in 2015 using multigap resistive plate chamber technology, providing a time resolution of 60 ps [47–49] and benefiting 82% of the data used in this analysis.

To determine the detection efficiency, simulated samples of 4×10^5 $e^+e^- \to \Xi^0\bar{\Xi}^0$ events are produced for each of the forty-five CM energy points from 3.51 to 4.95 GeV with GEANT4-

JHEP11(2024)062

based [50] Monte Carlo (MC) software, which includes the geometric description of the BESIII detector and the detector response [51]. The simulation models the beam energy spread and initial state radiation (ISR) in the e^+e^- annihilations with the generator KKMC [52]. The $e^+e^- \to \Xi^0\bar{\Xi}^0$ process and its subsequent decays are simulated with a uniform phase space (PHSP) model by EVTGEN [53, 54].

3 Event selection

Reconstructing $e^+e^- \to \Xi^0\bar{\Xi}^0$ candidate events fully has low efficiency. To achieve higher efficiency, a single baryon Ξ^0 tag technique is employed, i.e., only the Ξ^0 baryon is reconstructed via its decay $\Xi^0 \to \pi^0\Lambda$ with the subsequent decays $\Lambda \to p\pi^-$ and $\pi^0 \to \gamma\gamma$, and the antibaryon $\bar{\Xi}^0$ is identified in the Ξ^0 recoil mass distribution. The charge conjugate decays are implied unless otherwise noted.

Charged tracks are required to be within the angular coverage of the MDC: $|\cos\theta| < 0.93$, where θ is the polar angle with respect to the z-axis, which is the symmetry axis of the MDC. At least one positive and one negative charged track well reconstructed in the MDC are required.

Particle identification (PID) for charged tracks combines measurements of the specific ionization energy loss in the MDC (dE/dx) and the flight time in the TOF to form likelihoods $\mathcal{L}(h)$ ($h = p, K, \pi$) for each hadron h hypothesis. Tracks are identified as protons when the proton hypothesis has the greatest likelihood ($\mathcal{L}(p) > \mathcal{L}(K)$ and $\mathcal{L}(p) > \mathcal{L}(\pi)$), while charged pions are identified when $\mathcal{L}(\pi) > \mathcal{L}(K)$ and $\mathcal{L}(\pi) > \mathcal{L}(p)$. Events with at least one p and one π^- are kept for further analysis.

Photons are reconstructed from isolated showers in the EMC. The energy deposited in the nearby TOF counter is included to improve the reconstruction efficiency and energy resolution. The energies of photons are required to be greater than 25 MeV in the EMC barrel region ($|\cos\theta| < 0.8$), and greater than 50 MeV in the EMC end-cap region ($0.86 < |\cos\theta| < 0.92$). Furthermore, to suppress electronic noise and showers unrelated to the event, the difference between the EMC time and the event start time is required to be within [0, 700] ns. Events with at least two photons are kept for further analysis.

To reconstruct the π^0 meson from the $\Xi^0 \to \pi^0\Lambda$ decay, a one-constraint (1C) kinematic fit is applied to all $\gamma\gamma$ combinations under the hypothesis of $\pi^0 \to \gamma\gamma$, constraining the invariant mass of two photons to the π^0 mass, and $\chi^2_{\rm 1C} \leq 20$ is required to suppress the non-π^0 background [55–57].

To reconstruct the Λ candidate, a secondary vertex fit looping over all $p\pi^-$ combinations is employed, and the corresponding χ^2 value is required to be less than 500 by default. The distance between the interaction point and the decay vertex of the Λ candidate must be greater than zero. Further, a requirement of $|M_{p\pi^-} - m_\Lambda| \leq 5\,\mathrm{MeV}/c^2$ is imposed, where $M_{p\pi^-}$ is the invariant mass of the $p\pi^-$ combination and m_Λ is the Λ mass [58]. The requirement is determined by the figure-of-merit (FOM $= \mathcal{S}'/\sqrt{\mathcal{S}' + B}$), where $\mathcal{S}'$ is the number of signal MC events and B is the number of the estimated background events.

The Ξ^0 candidate with the minimum value of $|M_{\pi^0\Lambda} - m_{\Xi^0}|$ of all $\pi^0\Lambda$ combinations is selected, where $M_{\pi^0\Lambda}$ is the invariant mass of the $\pi^0\Lambda$ system, and m_{Ξ^0} is the Ξ^0 mass [58].

JHEP11(2024)062

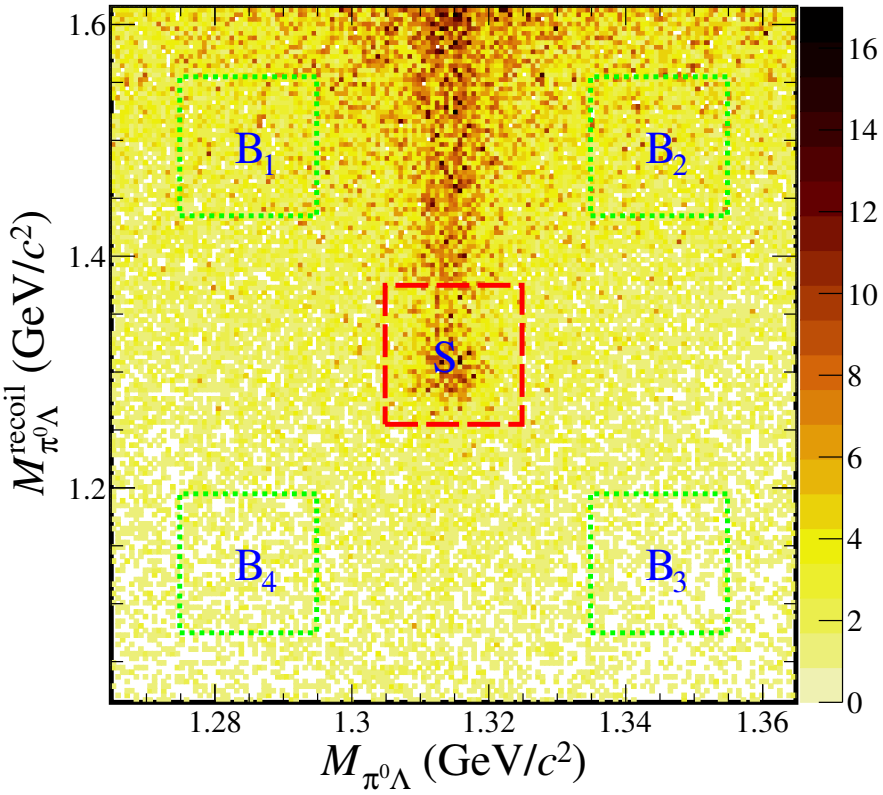

Figure 1. The distribution of $M^{\rm recoil}_{\pi^0\Lambda}$ versus $M_{\pi^0\Lambda}$ of the accepted candidates of data summed over CM energy points. The red box represents the signal region, and the green boxes represent sideband regions.

The mass recoiling against the selected $\pi^0\Lambda$ system is given by

$$M^{\rm recoil}_{\pi^0\Lambda} = \sqrt{\left(\sqrt{s} - E_{\pi^0\Lambda}\right)^2 - |\vec{p}_{\pi^0\Lambda}|^2}, \tag{3.1}$$

where $E_{\pi^0\Lambda}$ and $\vec{p}_{\pi^0\Lambda}$ are the energy and momentum, respectively, of the selected $\pi^0\Lambda$ candidate in the CM system. The anti-baryon $\bar{\Xi}^0$ candidate is required to be in the signal mass window $|M_{\pi^0\Lambda} - m_{\Xi^0}| \leq 10\,{\rm MeV}/c^2$ and $|M^{\rm recoil}_{\pi^0\Lambda} - m_{\Xi^0}| \leq 60\,{\rm MeV}/c^2$, marked by S as shown in figure 1. A clear accumulation around the Ξ^0 mass can be seen in figure 1. The $M^{\rm recoil}_{\pi^0\Lambda}$ tail from the $\gamma\Xi^0\bar{\Xi}^0$, $\gamma\gamma\Xi^0\bar{\Xi}^0$, and $\gamma\gamma\gamma\Xi^0\bar{\Xi}^0$ processes contribute negligibly to the signal yields.

4 Born cross section measurement

4.1 Determination of signal yields

After applying the above requirements, the remaining background events mainly come from the $e^+e^- \to \pi^0\pi^0\Lambda\Lambda$ process with the same final state as the signal channel. The background yields in the signal region are evaluated using four sideband regions B_i, where i runs over 1 to 4, each with the same area as the signal regions. The sideband regions are defined in the mass windows of $M_{\pi^0\Lambda}$ and $M^{\rm recoil}_{\pi^0\Lambda}$ as shown in figure 1, i.e., B_1: [1.275, 1.295] and [1.435,

JHEP11(2024)062

1.555] GeV/c^2, B_2: [1.335, 1.355] and [1.435, 1.555] GeV/c^2, B_3: [1.335, 1.355] and [1.075, 1.195] GeV/c^2, B_4: [1.275, 1.295] and [1.075, 1.195] GeV/c^2. The signal yield $N_{\rm obs}$ for the $e^+e^- \to \Xi^0\bar{\Xi}^0$ process at each CM energy point is then determined by $N_{\rm obs} = N_{\rm S} - N_{\rm bkg}$, where N_S represents the number of events in the signal region and $N_{\rm bkg}$ is the number of background events, i.e., $N_{\rm bkg} = \frac{1}{4}\sum_{i=1}^{4} N_{B_i}$. The uncertainty of $N_{\rm obs}$ and its upper limit are computed by the TRolke method [59]. The numerical results are summarized in table 1.

4.2 Determination of Born cross section and effective form factor

The Born cross section of the $e^+e^- \to \Xi^0\bar{\Xi}^0$ process is given by

$$\sigma^B = \frac{N_{\rm obs}}{2\mathcal{L}(1+\delta)\frac{1}{|1-\Pi|^2}\epsilon\mathcal{B}}, \tag{4.1}$$

where the factor of 2 accounts for the charge conjugate mode being included, $\mathcal{L}$ is the integrated luminosity, $(1+\delta)$ is the ISR correction factor, $\frac{1}{|1-\Pi|^2}$ is the vacuum polarization (VP) correction factor, ϵ is the detection efficiency, and $\mathcal{B}$ represents the products of the branching fractions of $\Xi^0 \to \pi^0\Lambda$, $\Lambda \to p\pi^-$ and $\pi^0 \to \gamma\gamma$ [58]. The VP correction factor is calculated according to ref. [60]. The results of the measured Born cross section for each CM energy point are listed in table 1. Note that the single-baryon tag method causes double counting of the $\Xi^0\bar{\Xi}^0$ final state. To correct for this effect, a factor of 1.08 is taken into account when calculating the statistical uncertainties based on the study of MC simulation [57]. The efficiency and ISR correction factor are obtained through an iterative process [66]. The measured Born cross section at each CM energy point is shown in figure 2 together with the results from the charged mode $e^+e^- \to \Xi^-\bar{\Xi}^+$ from the BESIII [31] and $\Xi^0\bar{\Xi}^0$ results from CLEO-c [43] measurements. Our results are roughly consistent with those of CLEO-c at $\sqrt{s} = 3.770$ and 4.160 GeV. Figure 2 also shows the energy dependence of the Ξ^0 effective form factor $G_{\rm eff}(s)$ compared with the CLEO-c results at $\sqrt{s} = 3.770$ and 4.160 GeV [43]. $|G_{\rm eff}(s)|$ is defined as [26]

$$|G_{\rm eff}(s)| = \sqrt{\frac{3s\sigma^B}{4\pi\alpha^2\beta\left(\frac{1}{2\tau}+1\right)}}, \tag{4.2}$$

where $\alpha = \frac{1}{137}$ is the fine structure constant, $\beta = \sqrt{1-\frac{1}{\tau}}$ is the velocity of Ξ^0 in CM system, $\tau = \frac{s}{4m^2_{\Xi^0}}$, and m_{Ξ^0} is the Ξ^0 mass [58]. Also shown in figure 2 are the ratios of Born cross sections and the effective form factors for the reactions of $e^+e^- \to \Xi^0\bar{\Xi}^0$ and $e^+e^- \to \Xi^-\bar{\Xi}^+$ from the BESIII experiment [31].

5 Systematic uncertainty

Systematic uncertainties on the Born cross section measurements mainly originate from the integrated luminosity, the Ξ^0 reconstruction, background, angular distribution, branching fractions, and input line shape.

5.1 Luminosity

The luminosity at each CM energy point is measured using Bhabha events, with an uncertainty of 1.0% [63], which is taken as the systematic uncertainty due to the luminosity measurement.

JHEP11(2024)062

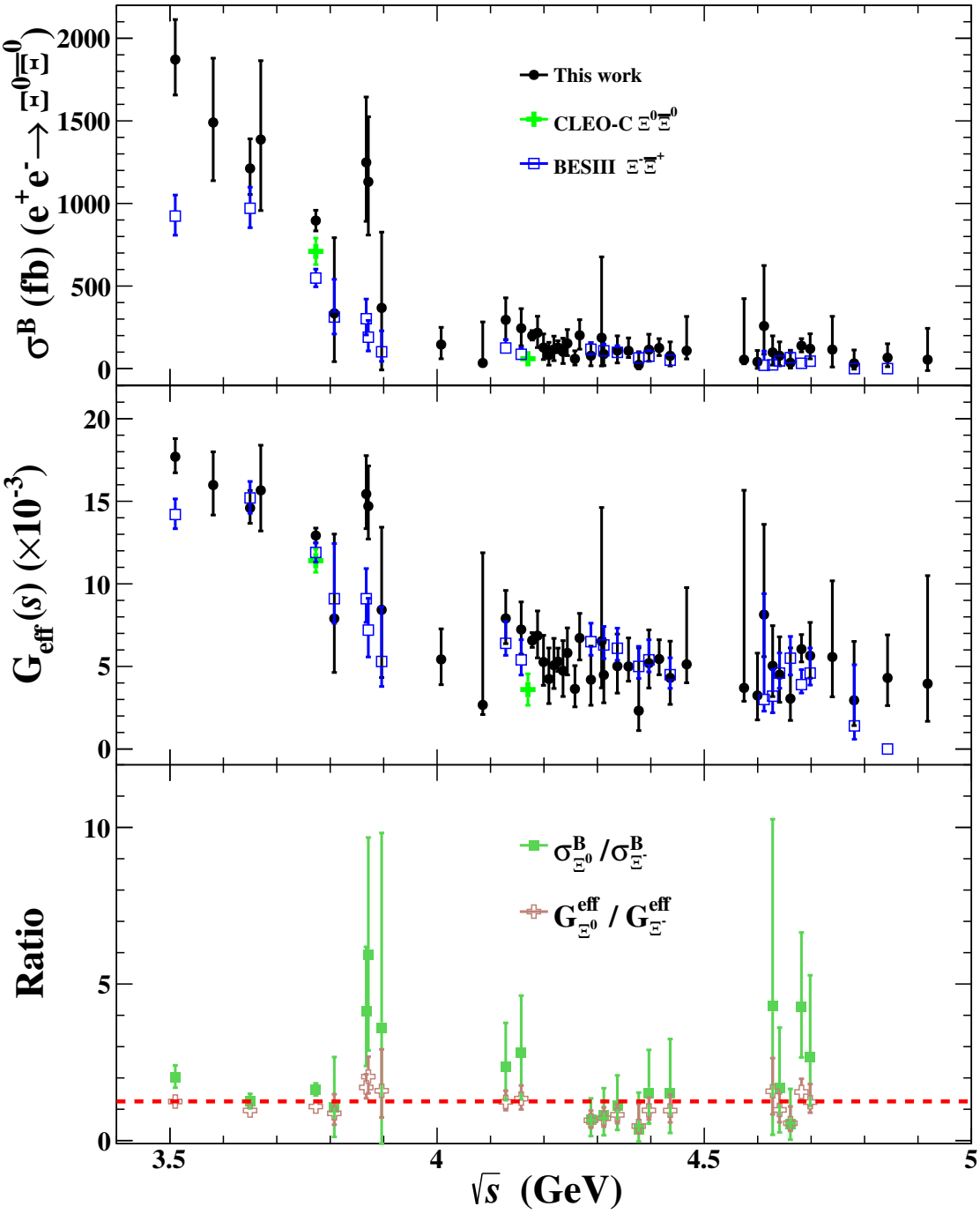

Figure 2. Comparisons of the Born cross section (σ^B) and the effective form factor ($G_{\rm eff}(s)$) for $e^+e^- \to \Xi^0\bar{\Xi}^0$ from this work and CLEO-c [43] with $e^+e^- \to \Xi^-\bar{\Xi}^+$ from BESIII [31] as a function of CM energy. The bottom one shows the ratios of the Born cross sections and the effective form factors for the reactions of $e^+e^- \to \Xi^0\bar{\Xi}^0$ and $e^+e^- \to \Xi^-\bar{\Xi}^+$, the red dashed line represents the theoretically predicted cross section ratio [40]. Here the uncertainties include both systematic and statistical uncertainties.

JHEP11(2024)062

$\sqrt{s}$ (GeV)	$\mathcal{L}$ (pb^{-1})	$\frac{1}{\lvert 1-\Pi\rvert^2}$	$\epsilon(1+\delta)$	$N_{\rm S}$	$N_{\rm bkg}$	$N_{\rm obs}$	σ^B (fb)	$\lvert G_{\rm eff}(s)\rvert$ ($\times 10^{-3}$)	$S(\sigma)$
3.51000	405.7	1.04	12.8	212	83.8	$128.3^{+12.6}_{-10.6}$	1871^{+199}_{-167} ±120	$17.7^{+0.9}_{-0.8}$ ±0.6	11.7
3.58100	85.7	1.04	13.0	39	17.3	$21.8^{+4.9}_{-4.4}$	1490^{+363}_{-326} ±96	$16.0^{+1.9}_{-1.7}$ ±0.5	4.6
3.65000	410.0	1.02	12.7	126	44.8	$81.3^{+9.8}_{-8.3}$	1212^{+158}_{-134} ±78	$14.6^{+0.9}_{-0.8}$ ±0.5	9.9
3.67000	84.7	0.99	12.5	26	7.8	$18.3^{+5.8}_{-5.2}$	1387^{+476}_{-427} ±89	$15.6^{+2.7}_{-2.4}$ ±0.5	5.1
3.77300	7926.8	1.06	12.2	2162	1004	$1158.0^{+35.0}_{-34.0}$	896^{+29}_{-28} ±56	$12.8^{+0.2}_{-0.2}$ ±0.4	8.1
3.80765	50.5	1.06	12.2	8	5.3	$2.8^{+3.3}_{-2.1}$ (<9.5)	334^{+433}_{-276} ±22 (<1159)	$7.9^{+5.1}_{-3.3}$ ±0.2 (<14.7)	1.4
3.86741	108.9	1.05	11.8	29	7.8	$21.3^{+5.8}_{-5.2}$	1249^{+368}_{-331} ±80	$15.4^{+2.3}_{-2.0}$ ±0.5	5.9
3.87131	110.3	1.05	11.7	25	5.8	$19.3^{+5.8}_{-4.7}$	1131^{+368}_{-298} ±73	$14.7^{+2.4}_{-1.9}$ ±0.5	5.9
3.89624	52.6	1.05	11.7	7	4.0	$3.0^{+3.3}_{-2.7}$ (<9.1)	368^{+437}_{-357} ±24 (<1119)	$8.4^{+5.0}_{-4.1}$ ±0.3 (<14.7)	1.6
4.00762	482.0	1.04	10.8	30	20.0	$10.0^{+6.3}_{-5.2}$ (<22.3)	146^{+99}_{-82} ±9 (<326)	$5.4^{+1.8}_{-1.5}$ ±0.2 (<8.1)	2.3
4.08545	52.9	1.05	10.4	2	1.8	$0.3^{+1.6}_{-0.1}$ (<4.6)	34^{+237}_{-15} ±2 (<632)	$2.7^{+9.2}_{-0.6}$ ±0.1 (<11.5)	0.6
4.12848	401.5	1.05	9.4	26	11.3	$14.8^{+5.8}_{-5.2}$	295^{+125}_{-112} ±19	$7.9^{+1.7}_{-1.5}$ ±0.3	3.8
4.15744	408.7	1.05	9.4	22	9.5	$12.5^{+5.3}_{-4.7}$	244^{+112}_{-99} ±16	$7.2^{+1.7}_{-1.5}$ ±0.2	3.6
4.17800	3189	1.05	9.7	154	72.3	$81.8^{+9.8}_{-8.3}$	200^{+26}_{-22} ±13	$6.6^{+0.4}_{-0.4}$ ±0.2	8.2
4.18800	526.7	1.05	9.5	27	12.5	$14.5^{+5.8}_{-5.2}$	217^{+94}_{-84} ±14	$6.9^{+1.5}_{-1.3}$ ±0.2	3.7
4.19915	526.0	1.06	9.5	17	8.5	$8.5^{+4.8}_{-4.2}$ (<18.0)	127^{+78}_{-68} ±8 (<271)	$5.3^{+1.6}_{-1.4}$ ±0.2 (<7.7)	2.7
4.20939	517.1	1.06	9.3	15	9.8	$5.3^{+4.3}_{-3.4}$ (<14.7)	82^{+73}_{-57} ±5 (<231)	$4.2^{+1.9}_{-1.5}$ ±0.1 (<7.1)	1.8
4.21893	514.6	1.06	9.0	15	7.8	$7.3^{+4.3}_{-3.7}$ (<16.5)	117^{+75}_{-65} ±8 (<267)	$5.1^{+1.6}_{-1.4}$ ±0.2 (<7.7)	2.5
4.22626	1100.9	1.06	9.4	40	22.5	$17.5^{+4.9}_{-3.5}$	127^{+39}_{-28} ±8	$5.3^{+0.8}_{-0.6}$ ±0.2	3.5
4.23570	530.3	1.06	9.4	18	11.3	$6.8^{+4.8}_{-4.1}$ (<16.5)	101^{+78}_{-67} ±7 (<249)	$4.7^{+1.8}_{-1.6}$ ±0.2 (<7.4)	2.1
4.24397	538.1	1.06	9.2	19	9.0	$10.0^{+4.8}_{-4.2}$	153^{+79}_{-69} ±10	$5.8^{+1.5}_{-1.3}$ ±0.2	3.0
4.25797	828.4	1.05	9.2	20	14.0	$6.0^{+4.3}_{-3.3}$ (<16.1)	59^{+46}_{-35} ±4 (<160)	$3.6^{+1.4}_{-1.1}$ ±0.1 (<6.0)	1.8
4.26681	531.1	1.05	9.1	21	8.0	$13.0^{+5.3}_{-4.7}$	202^{+89}_{-79} ±13	$6.7^{+1.5}_{-1.3}$ ±0.2	3.9
4.28788	502.4	1.05	8.2	11	6.8	$4.3^{+4.1}_{-3.1}$ (<12.4)	78^{+76}_{-58} ±5 (<229)	$4.2^{+2.0}_{-1.5}$ ±0.1 (<7.2)	1.7
4.30789	45.1	1.05	8.9	2	1.0	$1.0^{+2.3}_{-0.9}$ (<4.6)	187^{+465}_{-162} ±12 (<864)	$6.5^{+8.1}_{-2.8}$ ±0.2 (<14.0)	1.1
4.31205	501.2	1.05	8.1	13	8.3	$4.8^{+4.3}_{-3.3}$ (<13.1)	88^{+86}_{-66} ±6 (<244)	$4.5^{+2.2}_{-1.7}$ ±0.1 (<7.5)	1.8
4.33739	505.0	1.05	8.2	14	8.0	$6.0^{+4.6}_{-3.6}$ (<14.3)	109^{+85}_{-71} ±7 (<261)	$5.0^{+1.9}_{-1.6}$ ±0.2 (<7.8)	2.1
4.35826	543.9	1.05	8.7	12	5.3	$6.8^{+4.3}_{-2.2}$ (<14.5)	108^{+74}_{-38} ±7 (<232)	$5.0^{+1.7}_{-0.9}$ ±0.2 (<7.4)	2.7
4.37737	522.7	1.05	7.9	11	9.8	$1.3^{+3.8}_{-1.2}$ (<9.8)	23^{+75}_{-24} ±1 (<181)	$2.3^{+3.8}_{-1.2}$ ±0.1 (<7.8)	0.9
4.39645	507.8	1.05	7.8	12	6.0	$6.0^{+4.3}_{-3.2}$ (<13.7)	115^{+89}_{-66} ±7 (<262)	$5.2^{+2.0}_{-1.5}$ ±0.2 (<7.9)	2.3
4.41558	1090.7	1.05	8.2	29	14.3	$14.8^{+5.8}_{-4.7}$	125^{+53}_{-43} ±8	$5.4^{+1.2}_{-0.9}$ ±0.2	3.5
4.43624	569.9	1.05	7.7	15	10.5	$4.5^{+4.3}_{-3.1}$ (<13.7)	77^{+80}_{-58} ±5 (<238)	$4.3^{+2.2}_{-1.6}$ ±0.2 (<7.5)	1.6
4.46706	111.1	1.05	7.8	2	0.8	$1.3^{+2.1}_{-0.5}$ (<5.4)	108^{+197}_{-47} ±7 (<470)	$5.1^{+4.6}_{-1.1}$ ±0.2 (<18.0)	1.4
4.57450	48.9	1.05	7.1	1	0.8	$0.3^{+1.5}_{-0.1}$ (<3.7)	54^{+351}_{-23} ±3 (<803)	$3.7^{+12.0}_{-0.8}$ ±0.1 (<14.2)	0.6
4.59953	586.9	1.06	7.0	8	5.8	$2.3^{+3.3}_{-1.9}$ (<9.5)	41^{+65}_{-38} ±3 (<174)	$3.2^{+2.6}_{-1.5}$ ±0.1 (<6.7)	1.2
4.61186	103.7	1.05	6.3	4	1.8	$2.3^{+2.8}_{-1.3}$ (<7.5)	258^{+347}_{-162} ±17 (<863)	$8.1^{+5.5}_{-2.5}$ ±0.3 (<15.0)	1.6
4.62800	521.5	1.05	6.2	11	6.8	$4.3^{+3.8}_{-2.9}$ (<12.4)	98^{+95}_{-72} ±6 (<287)	$5.0^{+2.4}_{-1.9}$ ±0.2 (<8.6)	1.7
4.64091	551.7	1.05	6.1	8	4.5	$3.5^{+3.3}_{-2.4}$ (<10.4)	78^{+79}_{-58} ±5 (<233)	$4.5^{+2.3}_{-1.7}$ ±0.1 (<7.8)	1.7
4.66124	529.4	1.05	6.0	4	2.5	$1.5^{+2.8}_{-1.2}$ (<6.7)	36^{+72}_{-31} ±2 (<159)	$3.0^{+3.1}_{-1.3}$ ±0.1 (<6.4)	1.2
4.68192	1667.4	1.05	5.9	25	6.3	$18.3^{+4.8}_{-4.2}$	139^{+39}_{-34} ±9	$6.0^{+0.9}_{-0.8}$ ±0.2	5.7
4.69822	535.5	1.06	5.9	6	1.0	$5.0^{+3.3}_{-2.1}$	120^{+86}_{-57} ±8	$5.6^{+2.0}_{-1.3}$ ±0.2	3.4
4.73970	163.9	1.06	5.9	3	1.5	$1.5^{+2.3}_{-1.2}$ (<6.1)	115^{+191}_{-100} ±7 (<470)	$5.6^{+4.6}_{-2.4}$ ±0.2 (<11.2)	1.3
4.78054	511.5	1.06	5.7	5	3.8	$1.3^{+2.3}_{-1.2}$ (<7.2)	32^{+77}_{-33} ±2 (<184)	$2.9^{+3.6}_{-1.5}$ ±0.1 (<7.1)	1.0
4.84307	525.2	1.06	5.4	5	2.5	$2.5^{+2.8}_{-1.8}$ (<8.1)	66^{+80}_{-51} ±4 (<215)	$4.3^{+2.6}_{-1.7}$ ±0.1 (<7.7)	1.6
4.91802	207.8	1.06	5.0	3	2.3	$0.8^{+2.3}_{-0.8}$ (<5.3)	54^{+180}_{-62} ±3 (<384)	$3.9^{+6.5}_{-2.3}$ ±0.1 (<10.5)	0.8

Table 1. The Born cross section σ^B and the effective form factor $|G_{\rm eff}(s)|$ for $e^+e^- \to \Xi^0\bar{\Xi}^0$ at forty-five energy points between 3.51 and 4.95 GeV. The values in the brackets are the corresponding upper limits at the 90% C.L.. The first uncertainties are statistical, and the second are systematic. $\sqrt{s}$ is the e^+e^- CM energy [61, 62], $\mathcal{L}$ is the integrated luminosity of each data set [63–65], $\frac{1}{|1-\Pi|^2}$ is the vacuum polarization correction factor, and $\epsilon(1+\delta)$ is the product of the ISR correction factor and the detection efficiency. $N_{\rm S}$ is the number of events in the signal region, $N_{\rm bkg}$ is the number of background events scaled from the sideband region, and $N_{\rm obs}$ is the number of observed events after subtracting $N_{\rm bkg}$ from $N_{\rm S}$ with the uncertainty calculated by the TRolke method [59] (the number of signal events for the upper limit with the consideration of systematic uncertainty estimated based on the TRolke method [59]). σ^B is the Born cross section, $|G_{\rm eff}(s)|$ is the effective form factor, and S is the statistical significance.

JHEP11(2024)062

5.2 Ξ^0 reconstruction

The systematic uncertainty due to the Ξ^0 reconstruction efficiency, incorporating the tracking and PID efficiencies, the photon selection efficiency, the reconstruction efficiencies of Λ and π^0, the Λ decay lengths, and the mass windows of Λ and Ξ^0, is evaluated by a control sample of $\psi(3686) \to \Xi^0\bar{\Xi}^0$ with the same method as used in refs. [67–76]. The efficiency difference between data and MC simulation is found to be 4.5%, which is taken as the systematic uncertainty of the Ξ^0 reconstruction.

5.3 Background

The systematic uncertainty due to the background is estimated by shifting the sideband regions inward and outward by 10 MeV for $M_{\pi^0\Lambda}$ and 60 MeV for $M^{\rm recoil}_{\pi^0\Lambda}$ from the signal region with a standard of 3σ mass resolution, using the sum of all energy points. The resulting largest difference of 1.2% is taken as the systematic uncertainty due to the background.

5.4 Angular distribution

The uncertainty due to the angular distribution is estimated to be 3.5% by comparing the efficiency of the angular distribution from the phase space simulation with that incorporating the Ξ^0 transverse polarization and the spin correlation.

5.5 Branching fractions

The uncertainty for the product of the branching fractions of $\Lambda \to p\pi^-$ and $\pi^0 \to \gamma\gamma$ is 0.8% taken from the Particle Data Group (PDG) [58].

5.6 Input line shape

The uncertainty due to the input line shape of the cross section for determining the product of the ISR correction and the detection efficiency $(1+\delta)\cdot\epsilon$ is from two parts. One part is due to the statistical uncertainty of the input cross section line shape, which is estimated by varying the central value of the nominal input line shape within $\pm$ 1σ of the statistical uncertainty. The $(1+\delta)\cdot\epsilon$ values for each CM energy point are then recalculated. This process is repeated 100 times, and a Gaussian function is used to fit the $(1+\delta)\cdot\epsilon$ distribution. The width of the Gaussian function is taken as the corresponding systematic uncertainty. The other uncertainty arises from the resonance parameters which are fixed in the fit to the input cross section. The uncertainty from the line-shape description is estimated with an alternative input cross section line shape based on one resonance plus a power-law function. The $(1+\delta)\cdot\epsilon$ value for each of CM energy points is then recalculated, and the largest change is taken as the systematic uncertainty. The total systematic uncertainty for the input line shape is 2.4% by adding both contributions in quadrature.

5.7 Total systematic uncertainty

Assuming all sources are independent, the total systematic uncertainty on the cross section measurement of 6.4% is determined by adding these sources in quadrature.

JHEP11(2024)062

6 Fit to the dressed cross section

The potential resonances are searched for by analyzing the dressed cross section ($\sigma^{\rm dressed} = \frac{\sigma^B}{|1-\Pi|^2}$) of the $e^+e^- \to \Xi^0\bar{\Xi}^0$ reaction using the least χ^2 method $\chi^2 = \Delta X^T V^{-1} \Delta X$. Here V is the covariance matrix incorporating both the correlated and uncorrelated uncertainties among different CM energy points, and ΔX is the vector of residuals between the measured and the fitted cross sections. The diagonal elements of V are the sum of the statistical uncertainties and uncorrelated systematic uncertainties, added in quadrature. The off-diagonal elements of V are correlated systematic uncertainties including the luminosity, Ξ^0 reconstruction and branching fraction by assuming them to be fully correlated for each CM energy.

Assuming the line shape of the dressed cross section of the $e^+e^- \to \Xi^0\bar{\Xi}^0$ reaction includes a charmonium(-like) amplitude, i.e., $\psi(3770)$, $\psi(4040)$, $\psi(4160)$, $\psi(4230)$, $\psi(4360)$, $\psi(4415)$ or $\psi(4660)$, plus a continuum contribution, a fit with the coherent sum of a power law(PL) function plus a Breit-Wigner (BW) function

$$\sigma^{\rm dressed}\left(\sqrt{s}\right) = \left| c_0 \frac{\sqrt{P\left(\sqrt{s}\right)}}{\left(\sqrt{s}\right)^n} + e^{i\phi} BW\left(\sqrt{s}\right) \sqrt{\frac{P\left(\sqrt{s}\right)}{P(M)}} \right|^2, \tag{6.1}$$

is used. Here ϕ is the interference angle between the BW function

$$\mathrm{BW}\left(\sqrt{s}\right) = \frac{\sqrt{12\pi\Gamma_{ee}\mathcal{B}\Gamma}}{s - M^2 + iM\Gamma}, \tag{6.2}$$

and the PL function, c_0 and n are free parameters, $P(\sqrt{s})$ is the two-body PHSP factor ($P(\sqrt{s}) = \frac{\sqrt{(s-(m_{\Xi^0}+m_{\bar{\Xi}^0})^2)(s-(m_{\Xi^0}-m_{\bar{\Xi}^0})^2)}}{2\sqrt{s}}$), M and Γ are the resonance mass and total width, respectively, fixed according to the PDG values [58]. $\Gamma_{ee}\mathcal{B}$ is the product of the electronic partial width and the branching fraction for each assumed charmonium(-like) state decaying into the $\Xi^0\bar{\Xi}^0$ final state. Figure 3 shows fits to the dressed cross section by eq. (6.1) with a PL function only and with a single charmonium(-like) amplitude, fitted one at a time. The parameters with the PL function only are fitted to be $c_0 = 1.1 \pm 0.3, n = 7.7 \pm 0.2$. The parameters with the assumed charmonium(-like) amplitude combined with their multiple solutions are summarized in table 2, where the possible multiple solutions are evaluated based on a two-dimensional scan method which scans all the pairs of $\Gamma_{ee}B$ and ϕ in parameter space as shown in figure 4. The significance for each resonance considering the systematic uncertainty is calculated by comparing the change of χ^2/n.d.f with and without including the resonance in the fit, where n.d.f represents the number of degrees of freedom, and no significant resonance is found. Consequently, $\Gamma_{ee}\mathcal{B}$ and its upper limit at the 90% C.L. using a Bayesian approach [77] and including the systematic uncertainty for each assumed charmonium(-like) state decaying into the $\Xi^0\bar{\Xi}^0$ final state are listed in table 2.

7 Summary

In summary, using a total integrated luminosity of 30 fb^{-1} of e^+e^- collision data collected by the BESIII detector at BEPCII for CM energies between 3.51 and 4.95 GeV, we measure the Born cross sections and the effective form factors at forty-five CM energy points for

JHEP11(2024)062

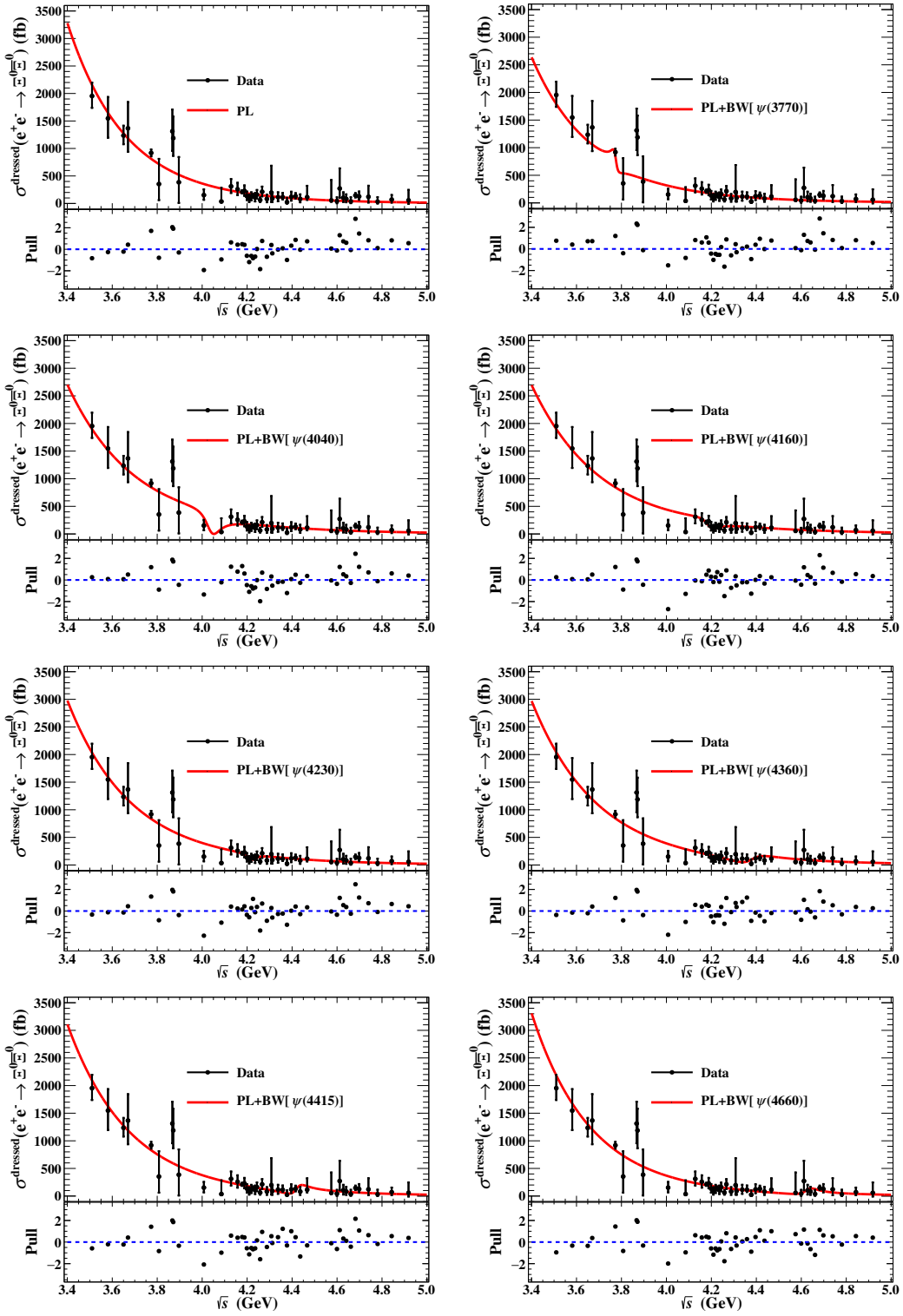

Figure 3. Fits to the dressed cross sections at CM energies from 3.51 to 4.95 GeV under the assumption of a PL function only (top left), or a PL function plus a resonance [i.e. $\psi(3770)$, $\psi(4040)$, $\psi(4160)$, $\psi(4230)$, $\psi(4360)$, $\psi(4415)$, or $\psi(4660)$]. Dots with error bars are the dressed cross sections, and the solid lines shows the fit results. The error bars include the statistical and systematic uncertainties summed in quadrature.

JHEP11(2024)062

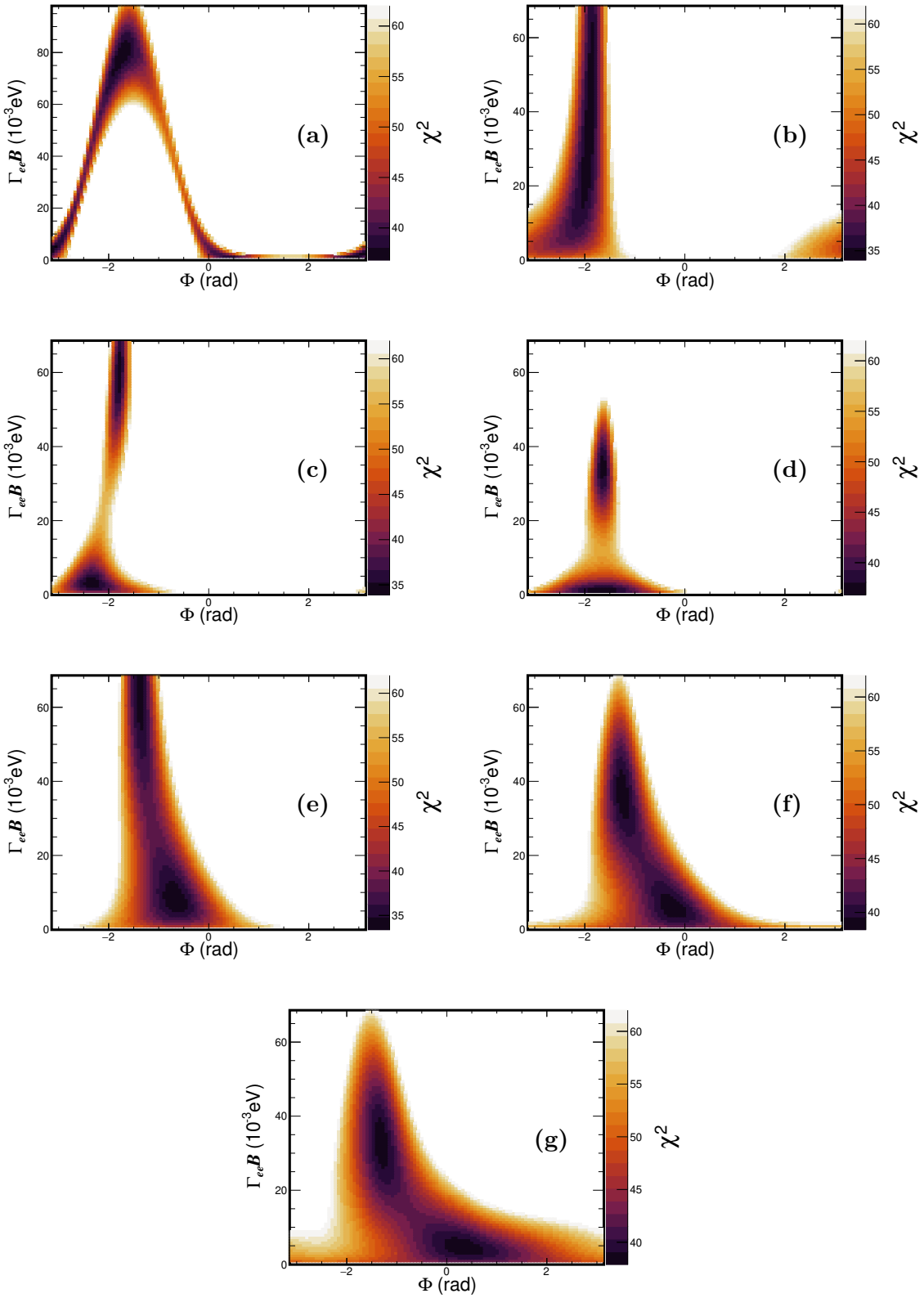

Figure 4. Contour distributions of χ^2 values in the $\Gamma_{ee}B - \Phi$ plane for (a) $\psi(3770)$, (b) $\psi(4040)$, (c) $\psi(4160)$, (d) $Y(4230)$, (e) $Y(4360)$, (f) $\psi(4415)$, and (g) $Y(4660)$ decaying into the $\Xi^0\bar{\Xi}^0$ final states.

JHEP11(2024)062

Parameter	Solution I	Solution II	χ^2/n.d.f
$\phi_{\psi(3770)}$	-1.7 ± 0.2	2.9 ± 0.8	
$\Gamma_{ee}\mathcal{B}_{\psi(3770)}$	79.1 ± 6.5 (< 89.0)	1.1 ± 3.3	$37/(45-4)$
$\phi_{\psi(4040)}$	-1.9 ± 0.1	–	
$\Gamma_{ee}\mathcal{B}_{\psi(4040)}$	34.2 ± 19.0 (< 83.4)	–	$34/(45-4)$
$\phi_{\psi(4160)}$	-1.8 ± 0.1	-2.3 ± 0.1	
$\Gamma_{ee}\mathcal{B}_{\psi(4160)}$	59.2 ± 3.8 (< 69.0)	3.0 ± 1.1	$34/(45-4)$
$\phi_{Y(4230)}$	-1.6 ± 0.1	-1.6 ± 0.2	
$\Gamma_{ee}\mathcal{B}_{Y(4230)}$	34.0 ± 2.7 (< 40.4)	1.0 ± 0.5	$37/(45-4)$
$\phi_{Y(4360)}$	-1.4 ± 0.1	-0.7 ± 0.2	
$\Gamma_{ee}\mathcal{B}_{Y(4360)}$	66.5 ± 8.1 (< 84.5)	7.9 ± 3.4	$34/(45-4)$
$\phi_{\psi(4415)}$	-1.2 ± 0.1	-0.2 ± 0.2	
$\Gamma_{ee}\mathcal{B}_{\psi(4415)}$	36.3 ± 5.0 (< 48.0)	5.6 ± 3.0	$39/(45-4)$
$\phi_{Y(4660)}$	-1.3 ± 0.1	0.3 ± 0.3	
$\Gamma_{ee}\mathcal{B}_{Y(4660)}$	32.8 ± 5.4 (< 45.0)	4.5 ± 1.9	$38/(45-4)$

Table 2. The fitted resonance parameters for $\Gamma_{ee}\mathcal{B}$ (10^{-3} eV) and ϕ (rad) with two solutions. The fit procedure includes both statistical and systematic uncertainties. Here χ^2/n.d.f indicates the fit quality for each assumed resonance.

the $e^+e^- \to \Xi^0\bar{\Xi}^0$ reaction. The dressed cross section of this reaction is fitted under the assumption of a single charmonium(-like) amplitude plus a continuum contribution. No obvious signal for any assumed charmonium(-like) state [i.e., $\psi(3770)$, $\psi(4040)$, $\psi(4160)$, $\psi(4230)$, $\psi(4360)$, $\psi(4415)$, or $\psi(4660)$] is found. The products of the branching fraction and electronic partial width for each assumed charmonium(-like) state decaying into the $\Xi^0\bar{\Xi}^0$ final state as well as the upper limits at the 90% C.L. are provided, which can be used to further constrain theoretical models [18, 23]. In addition, the ratios of the Born cross section and the effective form factor between this work and $e^+e^- \to \Xi^+\bar{\Xi}^-$, as shown in figure 2, can be used to test isospin symmetry and the vector meson dominance model [35–40]. The results of this study provide important experimental information on the correlation between vector charmonium(-like) states and the $e^+e^- \to \Xi^0\bar{\Xi}^0$ production.

Acknowledgments

The BESIII Collaboration thanks the staff of BEPCII and the IHEP computing center for their strong support. This work is supported in part by National Key R&D Program of China under Contracts Nos. 2023YFA1606000, 2020YFA0406300, 2020YFA0406400; National Natural Science Foundation of China (NSFC) under Contracts Nos. 12075107, 12247101, 11635010, 11735014, 11935015, 11935016, 11935018, 12025502, 12035009, 12035013, 12061131003, 12192260, 12192261, 12192262, 12192263, 12192264, 12192265, 12221005, 12225509, 12235017, 12361141819; the 111 Project under Grant No. B20063; the Chinese Academy of Sciences (CAS) Large-Scale Scientific Facility Program; the CAS Center for Excellence in Particle Physics (CCEPP); Joint Large-Scale Scientific Facility Funds of the NSFC and CAS under Contract No. U1832207; 100 Talents Program of CAS; The Institute of Nuclear and Particle

JHEP11(2024)062

Physics (INPAC) and Shanghai Key Laboratory for Particle Physics and Cosmology; German Research Foundation DFG under Contracts Nos. FOR5327, GRK 2149; Istituto Nazionale di Fisica Nucleare, Italy; Knut and Alice Wallenberg Foundation under Contracts Nos. 2021.0174, 2021.0299; Ministry of Development of Turkey under Contract No. DPT2006K-120470; National Research Foundation of Korea under Contract No. NRF-2022R1A2C1092335; National Science and Technology fund of Mongolia; National Science Research and Innovation Fund (NSRF) via the Program Management Unit for Human Resources & Institutional Development, Research and Innovation of Thailand under Contracts Nos. B16F640076, B50G670107; Polish National Science Centre under Contract No. 2019/35/O/ST2/02907; Swedish Research Council under Contract No. 2019.04595; The Swedish Foundation for International Cooperation in Research and Higher Education under Contract No. CH2018-7756; U.S. Department of Energy under Contract No. DE-FG02-05ER41374

References

[1] E598 collaboration, *Experimental Observation of a Heavy Particle J*, *Phys. Rev. Lett.* **33** (1974) 1404 [INSPIRE].

[2] SLAC-SP-017 collaboration, *Discovery of a Narrow Resonance in e^+e^- Annihilation*, *Phys. Rev. Lett.* **33** (1974) 1406 [INSPIRE].

[3] BES collaboration, *Measurements of the cross section for $e^+e^- \to$ hadrons at center-of-mass energies from 2 GeV to 5 GeV*, *Phys. Rev. Lett.* **88** (2002) 101802 [hep-ex/0102003] [INSPIRE].

[4] T. Barnes, S. Godfrey and E.S. Swanson, *Higher charmonia*, *Phys. Rev. D* **72** (2005) 054026 [hep-ph/0505002] [INSPIRE].

[5] BaBar collaboration, *Observation of a broad structure in the $\pi^+\pi^- J/\psi$ mass spectrum around 4.26 GeV/c^2*, *Phys. Rev. Lett.* **95** (2005) 142001 [hep-ex/0506081] [INSPIRE].

[6] BaBar collaboration, *Evidence of a broad structure at an invariant mass of 4.32 GeV/c^2 in the reaction $e^+e^- \to \pi^+\pi^-\psi(2S)$ measured at BaBar*, *Phys. Rev. Lett.* **98** (2007) 212001 [hep-ex/0610057] [INSPIRE].

[7] Belle collaboration, *Observation of Two Resonant Structures in $e^+e^- \to \pi^+\pi^-\psi(2S)$ via Initial State Radiation at Belle*, *Phys. Rev. Lett.* **99** (2007) 142002 [arXiv:0707.3699] [INSPIRE].

[8] Belle collaboration, *Measurement of $e^+e^- \to \pi^+\pi^- J/\psi$ cross section via initial state radiation at Belle*, *Phys. Rev. Lett.* **99** (2007) 182004 [arXiv:0707.2541] [INSPIRE].

[9] Belle collaboration, *Observation of a near-threshold enhancement in the $e^+e^- \to \Lambda_c^+\bar{\Lambda}_c^-$ cross section using initial-state radiation*, *Phys. Rev. Lett.* **101** (2008) 172001 [arXiv:0807.4458] [INSPIRE].

[10] BaBar collaboration, *Study of the reaction $e^+e^- \to J/\psi\pi^+\pi^-$ via initial-state radiation at BaBar*, *Phys. Rev. D* **86** (2012) 051102 [arXiv:1204.2158] [INSPIRE].

[11] Belle collaboration, *Study of $e^+e^- \to \pi^+\pi^- J/\psi$ and Observation of a Charged Charmoniumlike State at Belle*, *Phys. Rev. Lett.* **110** (2013) 252002 [*Erratum ibid.* **111** (2013) 019901] [arXiv:1304.0121] [INSPIRE].

JHEP11(2024)062

[12] BaBar collaboration, *Study of the reaction $e^+e^- \to \psi(2S)\pi^+\pi^-$ via initial-state radiation at BaBar*, *Phys. Rev. D* **89** (2014) 111103 [arXiv:1211.6271] [INSPIRE].

[13] Belle collaboration, *Measurement of $e^+e^- \to \pi^+\pi^-\psi(2S)$ via Initial State Radiation at Belle*, *Phys. Rev. D* **91** (2015) 112007 [arXiv:1410.7641] [INSPIRE].

[14] CLEO collaboration, *Charmonium decays of $Y(4260)$, $\psi(4160)$ and $\psi(4040)$*, *Phys. Rev. Lett.* **96** (2006) 162003 [hep-ex/0602034] [INSPIRE].

[15] BESIII collaboration, *$e^+e^- \to \omega\chi_{cJ}$ at center-of-mass energies from 4.21 to 4.42 GeV*, *Phys. Rev. Lett.* **114** (2015) 092003 [arXiv:1410.6538] [INSPIRE].

[16] BESIII collaboration, *Observation of Three Charmoniumlike States with $J^{PC} = 1^{--}$ in $e^+e^- \to D^{*0}D^{*-}\pi^+$*, *Phys. Rev. Lett.* **130** (2023) 121901 [arXiv:2301.07321] [INSPIRE].

[17] C.-Z. Yuan, *Charmonium and charmoniumlike states at the BESIII experiment*, *Natl. Sci. Rev.* **8** (2021) nwab182 [arXiv:2102.12044] [INSPIRE].

[18] F.E. Close and P.R. Page, *Gluonic charmonium resonances at BaBar and BELLE?*, *Phys. Lett. B* **628** (2005) 215 [hep-ph/0507199] [INSPIRE].

[19] N. Brambilla et al., *Heavy Quarkonium: Progress, Puzzles, and Opportunities*, *Eur. Phys. J. C* **71** (2011) 1534 [arXiv:1010.5827] [INSPIRE].

[20] R.A. Briceno et al., *Issues and Opportunities in Exotic Hadrons*, *Chin. Phys. C* **40** (2016) 042001 [arXiv:1511.06779] [INSPIRE].

[21] H.-X. Chen, W. Chen, X. Liu and S.-L. Zhu, *The hidden-charm pentaquark and tetraquark states*, *Phys. Rept.* **639** (2016) 1 [arXiv:1601.02092] [INSPIRE].

[22] J.-Z. Wang, D.-Y. Chen, X. Liu and T. Matsuki, *Constructing J/ψ family with updated data of charmoniumlike Y states*, *Phys. Rev. D* **99** (2019) 114003 [arXiv:1903.07115] [INSPIRE].

[23] R.-Q. Qian, Q. Huang and X. Liu, *Predicted $\Lambda\bar{\Lambda}$ and $\Xi^-\bar{\Xi}^+$ decay modes of the charmoniumlike $Y(4230)$*, *Phys. Lett. B* **833** (2022) 137292 [arXiv:2111.13821] [INSPIRE].

[24] B. Yan, C. Chen and J.-J. Xie, *Σ and Ξ electromagnetic form factors in the extended vector meson dominance model*, *Phys. Rev. D* **107** (2023) 076008 [arXiv:2301.00976] [INSPIRE].

[25] BESIII collaboration, *Search for Baryonic Decays of $\psi(3770)$ and $\psi(4040)$*, *Phys. Rev. D* **87** (2013) 112011 [arXiv:1305.1782] [INSPIRE].

[26] BESIII collaboration, *Measurement of the cross section for $e^+e^- \to \Xi^-\bar{\Xi}^+$ and observation of an excited Ξ baryon*, *Phys. Rev. Lett.* **124** (2020) 032002 [arXiv:1910.04921] [INSPIRE].

[27] BESIII collaboration, *Measurement of the cross section for $e^+e^- \to \Lambda\bar{\Lambda}$ and evidence of the decay $\psi(3770) \to \Lambda\bar{\Lambda}$*, *Phys. Rev. D* **104** (2021) L091104 [arXiv:2108.02410] [INSPIRE].

[28] BESIII collaboration, *Measurement of Λ baryon polarization in $e^+e^- \to \Lambda\bar{\Lambda}$ at $\sqrt{s} = 3.773$ GeV*, *Phys. Rev. D* **105** (2022) L011101 [arXiv:2111.11742] [INSPIRE].

[29] X. Wang and G. Huang, *Electromagnetic Form Factor of Doubly-Strange Hyperon*, *Symmetry* **14** (2022) 65 [INSPIRE].

[30] BESIII collaboration, *Study of $e^+e^- \to \Omega^-\bar{\Omega}^+$ at center-of-mass energies from 3.49 to 3.67 GeV*, *Phys. Rev. D* **107** (2023) 052003 [arXiv:2212.03693] [INSPIRE].

[31] BESIII collaboration, *Measurement of the cross section of $e^+e^- \to \Xi^-\overline{\Xi}^+$ at center-of-mass energies between 3.510 and 4.843 GeV*, *JHEP* **11** (2023) 228 [arXiv:2309.04215] [INSPIRE].

JHEP11(2024)062

[32] BESIII collaboration, *Measurement of Energy-Dependent Pair-Production Cross Section and Electromagnetic Form Factors of a Charmed Baryon*, *Phys. Rev. Lett.* **131** (2023) 191901 [arXiv:2307.07316] [INSPIRE].

[33] BESIII collaboration, *Measurement of Born cross section of $e^+e^- \to \Sigma^+\bar{\Sigma}^-$ at center-of-mass energies between 3.510 and 4.951 GeV*, *JHEP* **05** (2024) 022 [arXiv:2401.09468] [INSPIRE].

[34] BESIII collaboration, *Measurement of the cross sections of $e^+e^- \to K^-\bar{\Xi}^+\Lambda/\Sigma^0$ at center-of-mass energies between 3.510 and 4.914 GeV*, *JHEP* **07** (2024) 258 [arXiv:2406.18183] [INSPIRE].

[35] F. Iachello, A.D. Jackson and A. Lande, *Semiphenomenological fits to nucleon electromagnetic form-factors*, *Phys. Lett. B* **43** (1973) 191 [INSPIRE].

[36] F. Iachello and Q. Wan, *Structure of the nucleon from electromagnetic timelike form factors*, *Phys. Rev. C* **69** (2004) 055204 [nucl-th/0312074] [INSPIRE].

[37] R. Bijker and F. Iachello, *Re-analysis of the nucleon space- and time-like electromagnetic form-factors in a two-component model*, *Phys. Rev. C* **69** (2004) 068201 [nucl-th/0405028] [INSPIRE].

[38] Y. Yang, D.-Y. Chen and Z. Lu, *Electromagnetic form factors of Λ hyperon in the vector meson dominance model*, *Phys. Rev. D* **100** (2019) 073007 [arXiv:1902.01242] [INSPIRE].

[39] Z.-Y. Li, A.-X. Dai and J.-J. Xie, *Electromagnetic Form Factors of Λ Hyperon in the Vector Meson Dominance Model and a Possible Explanation of the Near-Threshold Enhancement of the Reaction*, *Chin. Phys. Lett.* **39** (2022) 011201 [arXiv:2107.10499] [INSPIRE].

[40] J.-P. Dai, X. Cao and H. Lenske, *Data driven isospin analysis of timelike octet baryons electromagnetic form factors and charmonium decay into baryon-anti-baryon*, *Phys. Lett. B* **846** (2023) 138192 [arXiv:2304.04913] [INSPIRE].

[41] BESIII collaboration, *Design and Construction of the BESIII Detector*, *Nucl. Instrum. Meth. A* **614** (2010) 345 [arXiv:0911.4960] [INSPIRE].

[42] C. Yu et al., *BEPCII Performance and Beam Dynamics Studies on Luminosity*, in the proceedings of the *7th International Particle Accelerator Conference*, Busan, South Korea, May 08–13 (2016) [DOI:10.18429/JACoW-IPAC2016-TUYA01] [INSPIRE].

[43] S. Dobbs et al., *Hyperon Form Factors & Diquark Correlations*, *Phys. Rev. D* **96** (2017) 092004 [arXiv:1708.09377] [INSPIRE].

[44] BESIII collaboration, *Future Physics Programme of BESIII*, *Chin. Phys. C* **44** (2020) 040001 [arXiv:1912.05983] [INSPIRE].

[45] J. Lu, Y. Xiao and X. Ji, *Online monitoring of the center-of-mass energy from real data at BESIII*, *Radiat. Detect. Technol. Methods* **4** (2020) 337.

[46] J.-W. Zhang et al., *Suppression of top-up injection backgrounds with offline event filter in the BESIII experiment*, *Radiat. Detect. Technol. Methods* **6** (2022) 289 [INSPIRE].

[47] X. Li et al., *Study of MRPC technology for BESIII endcap-TOF upgrade*, *Radiat. Detect. Technol. Methods* **1** (2017) 13 [INSPIRE].

[48] Y.-X. Guo et al., *The study of time calibration for upgraded end cap TOF of BESIII*, *Radiat. Detect. Technol. Methods* **1** (2017) 15 [INSPIRE].

[49] P. Cao et al., *Design and construction of the new BESIII endcap Time-of-Flight system with MRPC Technology*, *Nucl. Instrum. Meth. A* **953** (2020) 163053 [INSPIRE].

JHEP11(2024)062

[50] GEANT4 collaboration, *GEANT4 — a simulation toolkit*, *Nucl. Instrum. Meth. A* **506** (2003) 250 [INSPIRE].

[51] K.-X. Huang et al., *Method for detector description transformation to Unity and application in BESIII*, *Nucl. Sci. Tech.* **33** (2022) 142 [arXiv:2206.10117] [INSPIRE].

[52] S. Jadach, B.F.L. Ward and Z. Was, *Coherent exclusive exponentiation for precision Monte Carlo calculations*, *Phys. Rev. D* **63** (2001) 113009 [hep-ph/0006359] [INSPIRE].

[53] D.J. Lange, *The EvtGen particle decay simulation package*, *Nucl. Instrum. Meth. A* **462** (2001) 152 [INSPIRE].

[54] R.-G. Ping, *Event generators at BESIII*, *Chin. Phys. C* **32** (2008) 599 [INSPIRE].

[55] BESIII collaboration, *Study of J/ψ and $\psi(3686) \to \Sigma(1385)^0\bar{\Sigma}(1385)^0$ and $\Xi^0\bar{\Xi}^0$*, *Phys. Lett. B* **770** (2017) 217 [arXiv:1612.08664] [INSPIRE].

[56] BESIII collaboration, *Observation of $\psi(3686) \to \Xi(1530)^-\bar{\Xi}(1530)^+$ and $\Xi(1530)^-\bar{\Xi}^+$*, *Phys. Rev. D* **100** (2019) 051101 [arXiv:1907.13041] [INSPIRE].

[57] BESIII collaboration, *Measurement of cross section for $e^+e^- \to \Xi^0\bar{\Xi}^0$ near threshold*, *Phys. Lett. B* **820** (2021) 136557 [arXiv:2105.14657] [INSPIRE].

[58] Particle Data Group collaboration, *Review of particle physics*, *Phys. Rev. D* **110** (2024) 030001 [INSPIRE].

[59] J. Lundberg, J. Conrad, W. Rolke and A. Lopez, *Limits, discovery and cut optimization for a Poisson process with uncertainty in background and signal efficiency: TRolke 2.0*, *Comput. Phys. Commun.* **181** (2010) 683 [arXiv:0907.3450] [INSPIRE].

[60] F. Jegerlehner and R. Szafron, *$\rho^0 - \gamma$ mixing in the neutral channel pion form factor F_π^e and its role in comparing e^+e^- with τ spectral functions*, *Eur. Phys. J. C* **71** (2011) 1632 [arXiv:1101.2872] [INSPIRE].

[61] BESIII collaboration, *Measurement of the center-of-mass energies at BESIII via the di-muon process*, *Chin. Phys. C* **40** (2016) 063001 [arXiv:1510.08654] [INSPIRE].

[62] BESIII collaboration, *Measurements of the center-of-mass energies of collisions at BESIII*, *Chin. Phys. C* **45** (2021) 103001 [arXiv:2012.14750] [INSPIRE].

[63] BESIII collaboration, *Precision measurement of the integrated luminosity of the data taken by BESIII at center of mass energies between 3.810 GeV and 4.600 GeV*, *Chin. Phys. C* **39** (2015) 093001 [arXiv:1503.03408] [INSPIRE].

[64] BESIII collaboration, *Measurement of integrated luminosities at BESIII for data samples at center-of-mass energies between 4.0 and 4.6 GeV*, *Chin. Phys. C* **46** (2022) 113002 [arXiv:2203.03133] [INSPIRE].

[65] BESIII collaboration, *Luminosities and energies of e^+e^- collision data taken between 4.61 GeV and 4.95 GeV at BESIII*, *Chin. Phys. C* **46** (2022) 113003 [arXiv:2205.04809] [INSPIRE].

[66] W. Sun et al., *An iterative weighting method to apply ISR correction to e^+e^- hadronic cross-section measurements*, *Front. Phys. (Beijing)* **16** (2021) 64501 [arXiv:2011.07889] [INSPIRE].

[67] BESIII collaboration, *Measurements of baryon pair decays of χ_{cJ} mesons*, *Phys. Rev. D* **87** (2013) 032007 [*Erratum ibid.* **87** (2013) 059901] [arXiv:1211.2283] [INSPIRE].

[68] BESIII collaboration, *Study of ψ decays to the $\Xi^-\bar{\Xi}^+$ and $\Sigma(1385)^\mp\bar{\Sigma}(1385)^\pm$ final states*, *Phys. Rev. D* **93** (2016) 072003 [arXiv:1602.06754] [INSPIRE].

JHEP11(2024)062

[69] BESIII collaboration, *Observation of* $\psi(3686) \to \Xi(1530)^0\bar{\Xi}(1530)^0$ *and* $\Xi(1530)^0\bar{\Xi}^0$, *Phys. Rev. D* **104** (2021) 092012 [arXiv:2109.06621] [INSPIRE].

[70] BESIII collaboration, *Measurement of cross section for* $e^+e^- \to \Xi^-\bar{\Xi}^+$ *near threshold at BESIII*, *Phys. Rev. D* **103** (2021) 012005 [arXiv:2010.08320] [INSPIRE].

[71] BESIII collaboration, *Study of the processes* $\chi_{cJ} \to \Xi^-\bar{\Xi}^+$ *and* $\Xi^0\bar{\Xi}^0$, *JHEP* **06** (2022) 074 [arXiv:2202.08058] [INSPIRE].

[72] BESIII collaboration, *Observation of* Ξ^- *hyperon transverse polarization in* $\psi(3686) \to \Xi^-\bar{\Xi}^+$, *Phys. Rev. D* **106** (2022) L091101 [arXiv:2206.10900] [INSPIRE].

[73] BESIII collaboration, *First simultaneous measurement of* Ξ^0 *and* $\bar{\Xi}^0$ *asymmetry parameters in* $\psi(3686)$ *decay*, *Phys. Rev. D* **108** (2023) L011101 [arXiv:2302.09767] [INSPIRE].

[74] BESIII collaboration, *Measurement of* Λ *transverse polarization in* e^+e^- *collisions at* $\sqrt{s} = 3.68$–*3.71 GeV*, *JHEP* **10** (2023) 081 [*Erratum ibid.* **12** (2023) 080] [arXiv:2303.00271] [INSPIRE].

[75] BESIII collaboration, *Measurement of* Σ^+ *transverse polarization in* e^+e^- *collisions at* $\sqrt{s} = 3.68$–*3.71 GeV*, arXiv:2408.03205 [INSPIRE].

[76] BESIII collaboration, *Partial wave analysis of* $\psi(3686) \to \Lambda\bar{\Sigma}^0\pi^0 + c.c.$, arXiv:2408.00495 [INSPIRE].

[77] Y.-S. Zhu, *Bayesian credible interval construction for Poisson statistics*, *Chin. Phys. C* **32** (2008) 363 [arXiv:0812.2705] [INSPIRE].

JHEP11(2024)062

The BESIII collaboration

M. Ablikim[1], M.N. Achasov[4,c], P. Adlarson[76], O. Afedulidis[3], X.C. Ai[81], R. Aliberti[35], A. Amoroso[75A,75C], Y. Bai[57], O. Bakina[36], I. Balossino[29A], Y. Ban[46,h], H.-R. Bao[64], V. Batozskaya[1,44], K. Begzsuren[32], N. Berger[35], M. Berlowski[44], M. Bertani[28A], D. Bettoni[29A], F. Bianchi[75A,75C], E. Bianco[75A,75C], A. Bortone[75A,75C], I. Boyko[36], R.A. Briere[5], A. Brueggemann[69], H. Cai[77], X. Cai[1,58], A. Calcaterra[28A], G.F. Cao[1,64], N. Cao[1,64], S.A. Cetin[62A], X.Y. Chai[46,h], J.F. Chang[1,58], G.R. Che[43], Y.Z. Che[1,58,64], G. Chelkov[36,b], C. Chen[43], C.H. Chen[9], Chao Chen[55], G. Chen[1], H.S. Chen[1,64], H.Y. Chen[20], M.L. Chen[1,58,64], S.J. Chen[42], S.L. Chen[45], S.M. Chen[61], T. Chen[1,64], X.R. Chen[31,64], X.T. Chen[1,64], Y.B. Chen[1,58], Y.Q. Chen[34], Z.J. Chen[25,i], Z.Y. Chen[1,64], S.K. Choi[10], G. Cibinetto[29A], F. Cossio[75C], J.J. Cui[50], H.L. Dai[1,58], J.P. Dai[79], A. Dbeyssi[18], R.E. de Boer[3], D. Dedovich[36], C.Q. Deng[73], Z.Y. Deng[1], A. Denig[35], I. Denysenko[36], M. Destefanis[75A,75C], F. De Mori[75A,75C], B. Ding[67,1], X.X. Ding[46,h], Y. Ding[40], Y. Ding[34], J. Dong[1,58], L.Y. Dong[1,64], M.Y. Dong[1,58,64], X. Dong[77], M.C. Du[1], S.X. Du[81], Y.Y. Duan[55], Z.H. Duan[42], P. Egorov[36,b], Y.H. Fan[45], J. Fang[1,58], J. Fang[59], S.S. Fang[1,64], W.X. Fang[1], Y. Fang[1], Y.Q. Fang[1,58], R. Farinelli[29A], L. Fava[75B,75C], F. Feldbauer[3], G. Felici[28A], C.Q. Feng[72,58], J.H. Feng[59], Y.T. Feng[72,58], M. Fritsch[3], C.D. Fu[1], J.L. Fu[64], Y.W. Fu[1,64], H. Gao[64], X.B. Gao[41], Y.N. Gao[46,h], Yang Gao[72,58], S. Garbolino[75C], I. Garzia[29A,29B], L. Ge[81], P.T. Ge[19], Z.W. Ge[42], C. Geng[59], E.M. Gersabeck[68], A. Gilman[70], K. Goetzen[13], L. Gong[40], W.X. Gong[1,58], W. Gradl[35], S. Gramigna[29A,29B], M. Greco[75A,75C], M.H. Gu[1,58], Y.T. Gu[15], C.Y. Guan[1,64], A.Q. Guo[31,64], L.B. Guo[41], M.J. Guo[50], R.P. Guo[49], Y.P. Guo[12,g], A. Guskov[36,b], J. Gutierrez[27], K.L. Han[64], T.T. Han[1], F. Hanisch[3], X.Q. Hao[19], F.A. Harris[66], K.K. He[55], K.L. He[1,64], F.H. Heinsius[3], C.H. Heinz[35], Y.K. Heng[1,58,64], C. Herold[60], T. Holtmann[3], P.C. Hong[34], G.Y. Hou[1,64], X.T. Hou[1,64], Y.R. Hou[64], Z.L. Hou[1], B.Y. Hu[59], H.M. Hu[1,64], J.F. Hu[56,j], Q.P. Hu[72,58], S.L. Hu[12,g], T. Hu[1,58,64], Y. Hu[1], G.S. Huang[72,58], K.X. Huang[59], L.Q. Huang[31,64], X.T. Huang[50], Y.P. Huang[1], Y.S. Huang[59], T. Hussain[74], F. Hölzken[3], N. Hüsken[35], N. in der Wiesche[69], J. Jackson[27], S. Janchiv[32], J.H. Jeong[10], Q. Ji[1], Q.P. Ji[19], W. Ji[1,64], X.B. Ji[1,64], X.L. Ji[1,58], Y.Y. Ji[50], X.Q. Jia[50], Z.K. Jia[72,58], D. Jiang[1,64], H.B. Jiang[77], P.C. Jiang[46,h], S.S. Jiang[39], T.J. Jiang[16], X.S. Jiang[1,58,64], Y. Jiang[64], J.B. Jiao[50], J.K. Jiao[34], Z. Jiao[23], S. Jin[42], Y. Jin[67], M.Q. Jing[1,64], X.M. Jing[64], T. Johansson[76], S. Kabana[33], N. Kalantar-Nayestanaki[65], X.L. Kang[9], X.S. Kang[40], M. Kavatsyuk[65], B.C. Ke[81], V. Khachatryan[27], A. Khoukaz[69], R. Kiuchi[1], O.B. Kolcu[62A], B. Kopf[3], M. Kuessner[3], X. Kui[1,64], N. Kumar[26], A. Kupsc[44,76], W. Kühn[37], L. Lavezzi[75A,75C], T.T. Lei[72,58], Z.H. Lei[72,58], M. Lellmann[35], T. Lenz[35], C. Li[47], C. Li[43], C.H. Li[39], Cheng Li[72,58], D.M. Li[81], F. Li[1,58], G. Li[1], H.B. Li[1,64], H.J. Li[19], H.N. Li[56,j], Hui Li[43], J.R. Li[61], J.S. Li[59], K. Li[1], K.L. Li[19], L.J. Li[1,64], L.K. Li[1], Lei Li[48], M.H. Li[43], P.R. Li[38,k,l], Q.M. Li[1,64], Q.X. Li[50], R. Li[17,31], S.X. Li[12], T. Li[50], W.D. Li[1,64], W.G. Li[1,a], X. Li[1,64], X.H. Li[72,58], X.L. Li[50], X.Y. Li[1,8], X.Z. Li[59], Y.G. Li[46,h], Z.J. Li[59], Z.Y. Li[79], C. Liang[42], H. Liang[1,64], H. Liang[72,58], Y.F. Liang[54], Y.T. Liang[31,64], G.R. Liao[14], Y.P. Liao[1,64], J. Libby[26], A. Limphirat[60], C.C. Lin[55], C.X. Lin[64], D.X. Lin[31,64], T. Lin[1], B.J. Liu[1], B.X. Liu[77], C. Liu[34], C.X. Liu[1], F. Liu[1], F.H. Liu[53], Feng Liu[6], G.M. Liu[56,j], H. Liu[38,k,l], H.B. Liu[15], H.H. Liu[1], H.M. Liu[1,64], Huihui Liu[21], J.B. Liu[72,58], J.Y. Liu[1,64], K. Liu[38,k,l], K.Y. Liu[40], Ke Liu[22], L. Liu[72,58], Liang Liu[38,k,l], L.C. Liu[43], Lu Liu[43], M.H. Liu[12,g], P.L. Liu[1], Q. Liu[64], S.B. Liu[72,58], T. Liu[12,g], W.K. Liu[43], W.M. Liu[72,58], X. Liu[39], X. Liu[38,k,l], Y. Liu[81], Y. Liu[38,k,l], Y.B. Liu[43], Z.A. Liu[1,58,64], Z.D. Liu[9], Z.Q. Liu[50], X.C. Lou[1,58,64], F.X. Lu[59], H.J. Lu[23], J.G. Lu[1,58], X.L. Lu[1], Y. Lu[7], Y.P. Lu[1,58], Z.H. Lu[1,64], C.L. Luo[41], J.R. Luo[59], M.X. Luo[80], T. Luo[12,g], X.L. Luo[1,58], X.R. Lyu[64],

JHEP11(2024)062

Y.F. Lyu[43], F.C. Ma[40], H. Ma[79], H.L. Ma[1], J.L. Ma[1,64], L.L. Ma[50], L.R. Ma[67], M.M. Ma[1,64], Q.M. Ma[1], R.Q. Ma[1,64], T. Ma[72,58], X.T. Ma[1,64], X.Y. Ma[1,58], Y.M. Ma[31], F.E. Maas[18], I. MacKay[70], M. Maggiora[75A,75C], S. Malde[70], Y.J. Mao[46,h], Z.P. Mao[1], S. Marcello[75A,75C], Z.X. Meng[67], J.G. Messchendorp[13,65], G. Mezzadri[29A], H. Miao[1,64], T.J. Min[42], R.E. Mitchell[27], X.H. Mo[1,58,64], B. Moses[27], N. Yu. Muchnoi[4,c], J. Muskalla[35], Y. Nefedov[36], F. Nerling[18,e], L.S. Nie[20], I.B. Nikolaev[4,c], Z. Ning[1,58], S. Nisar[11,m], Q.L. Niu[38,k,l], W.D. Niu[55], Y. Niu [50], S.L. Olsen[64], S.L. Olsen[10,64], Q. Ouyang[1,58,64], S. Pacetti[28B,28C], X. Pan[55], Y. Pan[57], A. Pathak[34], Y.P. Pei[72,58], M. Pelizaeus[3], H.P. Peng[72,58], Y.Y. Peng[38,k,l], K. Peters[13,e], J.L. Ping[41], R.G. Ping[1,64], S. Plura[35], V. Prasad[33], F.Z. Qi[1], H. Qi[72,58], H.R. Qi[61], M. Qi[42], T.Y. Qi[12,g], S. Qian[1,58], W.B. Qian[64], C.F. Qiao[64], X.K. Qiao[81], J.J. Qin[73], L.Q. Qin[14], L.Y. Qin[72,58], X.P. Qin[12,g], X.S. Qin[50], Z.H. Qin[1,58], J.F. Qiu[1], Z.H. Qu[73], C.F. Redmer[35], K.J. Ren[39], A. Rivetti[75C], M. Rolo[75C], G. Rong[1,64], Ch. Rosner[18], M.Q. Ruan[1,58], S.N. Ruan[43], N. Salone[44], A. Sarantsev[36,d], Y. Schelhaas[35], K. Schoenning[76], M. Scodeggio[29A], K.Y. Shan[12,g], W. Shan[24], X.Y. Shan[72,58], Z.J. Shang[38,k,l], J.F. Shangguan[16], L.G. Shao[1,64], M. Shao[72,58], C.P. Shen[12,g], H.F. Shen[1,8], W.H. Shen[64], X.Y. Shen[1,64], B.A. Shi[64], H. Shi[72,58], J.L. Shi[12,g], J.Y. Shi[1], Q.Q. Shi[55], S.Y. Shi[73], X. Shi[1,58], J.J. Song[19], T.Z. Song[59], W.M. Song[34,1], Y.J. Song[12,g], Y.X. Song[46,h,n], S. Sosio[75A,75C], S. Spataro[75A,75C], F. Stieler[35], S. S Su[40], Y.J. Su[64], G.B. Sun[77], G.X. Sun[1], H. Sun[64], H.K. Sun[1], J.F. Sun[19], K. Sun[61], L. Sun[77], S.S. Sun[1,64], T. Sun[51,f], W.Y. Sun[34], Y. Sun[9], Y.J. Sun[72,58], Y.Z. Sun[1], Z.Q. Sun[1,64], Z.T. Sun[50], C.J. Tang[54], G.Y. Tang[1], J. Tang[59], M. Tang[72,58], Y.A. Tang[77], L.Y. Tao[73], Q.T. Tao[25,i], M. Tat[70], J.X. Teng[72,58], V. Thoren[76], W.H. Tian[59], Y. Tian[31,64], Z.F. Tian[77], I. Uman[62B], Y. Wan[55], S.J. Wang[50], B. Wang[1], B.L. Wang[64], Bo Wang[72,58], D.Y. Wang[46,h], F. Wang[73], H.J. Wang[38,k,l], J.J. Wang[77], J.P. Wang [50], K. Wang[1,58], L.L. Wang[1], M. Wang[50], N.Y. Wang[64], S. Wang[12,g], S. Wang[38,k,l], T. Wang[12,g], T.J. Wang[43], W. Wang[59], W. Wang[73], W.P. Wang[35,58,72,o], X. Wang[46,h], X.F. Wang[38,k,l], X.J. Wang[39], X.L. Wang[12,g], X.N. Wang[1], Y. Wang[61], Y.D. Wang[45], Y.F. Wang[1,58,64], Y.H. Wang[38,k,l], Y.L. Wang[19], Y.N. Wang[45], Y.Q. Wang[1], Yaqian Wang[17], Yi Wang[61], Z. Wang[1,58], Z.L. Wang[73], Z.Y. Wang[1,64], Ziyi Wang[64], D.H. Wei[14], F. Weidner[69], S.P. Wen[1], Y.R. Wen[39], U. Wiedner[3], G. Wilkinson[70], M. Wolke[76], L. Wollenberg[3], C. Wu[39], J.F. Wu[1,8], L.H. Wu[1], L.J. Wu[1,64], X. Wu[12,g], X.H. Wu[34], Y. Wu[72,58], Y.H. Wu[55], Y.J. Wu[31], Z. Wu[1,58], L. Xia[72,58], X.M. Xian[39], B.H. Xiang[1,64], T. Xiang[46,h], D. Xiao[38,k,l], G.Y. Xiao[42], S.Y. Xiao[1], Y.L. Xiao[12,g], Z.J. Xiao[41], C. Xie[42], X.H. Xie[46,h], Y. Xie[50], Y.G. Xie[1,58], Y.H. Xie[6], Z.P. Xie[72,58], T.Y. Xing[1,64], C.F. Xu[1,64], C.J. Xu[59], G.F. Xu[1], H.Y. Xu[67,2], M. Xu[72,58], Q.J. Xu[16], Q.N. Xu[30], W. Xu[1], W.L. Xu[67], X.P. Xu[55], Y. Xu[40], Y.C. Xu[78], Z.S. Xu[64], F. Yan[12,g], L. Yan[12,g], W.B. Yan[72,58], W.C. Yan[81], X.Q. Yan[1,64], H.J. Yang[51,f], H.L. Yang[34], H.X. Yang[1], J.H. Yang[42], T. Yang[1], Y. Yang[12,g], Y.F. Yang[1,64], Y.F. Yang[43], Y.X. Yang[1,64], Z.W. Yang[38,k,l], Z.P. Yao[50], M. Ye[1,58], M.H. Ye[8], J.H. Yin[1], Junhao Yin[43], Z.Y. You[59], B.X. Yu[1,58,64], C.X. Yu[43], G. Yu[1,64], J.S. Yu[25,i], M.C. Yu[40], T. Yu[73], X.D. Yu[46,h], Y.C. Yu[81], C.Z. Yuan[1,64], J. Yuan[34], J. Yuan[45], L. Yuan[2], S.C. Yuan[1,64], Y. Yuan[1,64], Z.Y. Yuan[59], C.X. Yue[39], A.A. Zafar[74], F.R. Zeng[50], S.H. Zeng[63A,63B,63C,63D], X. Zeng[12,g], Y. Zeng[25,i], Y.J. Zeng[1,64], Y.J. Zeng[59], X.Y. Zhai[34], Y.C. Zhai[50], Y.H. Zhan[59], A.Q. Zhang[1,64], B.L. Zhang[1,64], B.X. Zhang[1], D.H. Zhang[43], G.Y. Zhang[19], H. Zhang[81], H. Zhang[72,58], H.C. Zhang[1,58,64], H.H. Zhang[59], H.H. Zhang[34], H.Q. Zhang[1,58,64], H.R. Zhang[72,58], H.Y. Zhang[1,58], J. Zhang[81], J. Zhang[59], J.J. Zhang[52], J.L. Zhang[20], J.Q. Zhang[41], J.S. Zhang[12,g], J.W. Zhang[1,58,64], J.X. Zhang[38,k,l], J.Y. Zhang[1], J.Z. Zhang[1,64], Jianyu Zhang[64], L.M. Zhang[61], Lei Zhang[42], P. Zhang[1,64],

JHEP11(2024)062

Q.Y. Zhang[34], R.Y. Zhang[38,k,l], S.H. Zhang[1,64], Shulei Zhang[25,i], X.M. Zhang[1], X. Y Zhang[40], X.Y. Zhang[50], Y. Zhang[1], Y. Zhang[73], Y.T. Zhang[81], Y.H. Zhang[1,58], Y.M. Zhang[39], Yan Zhang[72,58], Z.D. Zhang[1], Z.H. Zhang[1], Z.L. Zhang[34], Z.Y. Zhang[77], Z.Y. Zhang[43], Z.Z. Zhang[45], G. Zhao[1], J.Y. Zhao[1,64], J.Z. Zhao[1,58], L. Zhao[1], Lei Zhao[72,58], M.G. Zhao[43], N. Zhao[79], R.P. Zhao[64], S.J. Zhao[81], Y.B. Zhao[1,58], Y.X. Zhao[31,64], Z.G. Zhao[72,58], A. Zhemchugov[36,b], B. Zheng[73], B.M. Zheng[34], J.P. Zheng[1,58], W.J. Zheng[1,64], Y.H. Zheng[64], B. Zhong[41], X. Zhong[59], H. Zhou[50], J.Y. Zhou[34], L.P. Zhou[1,64], S. Zhou[6], X. Zhou[77], X.K. Zhou[6], X.R. Zhou[72,58], X.Y. Zhou[39], Y.Z. Zhou[12,g], Z.C. Zhou[20], A.N. Zhu[64], J. Zhu[43], K. Zhu[1], K.J. Zhu[1,58,64], K.S. Zhu[12,g], L. Zhu[34], L.X. Zhu[64], S.H. Zhu[71], T.J. Zhu[12,g], W.D. Zhu[41], Y.C. Zhu[72,58], Z.A. Zhu[1,64], J.H. Zou[1], J. Zu[72,58]

[1] *Institute of High Energy Physics, Beijing 100049, People's Republic of China*
[2] *Beihang University, Beijing 100191, People's Republic of China*
[3] *Bochum Ruhr-University, D-44780 Bochum, Germany*
[4] *Budker Institute of Nuclear Physics SB RAS (BINP), Novosibirsk 630090, Russia*
[5] *Carnegie Mellon University, Pittsburgh, Pennsylvania 15213, U.S.A.*
[6] *Central China Normal University, Wuhan 430079, People's Republic of China*
[7] *Central South University, Changsha 410083, People's Republic of China*
[8] *China Center of Advanced Science and Technology, Beijing 100190, People's Republic of China*
[9] *China University of Geosciences, Wuhan 430074, People's Republic of China*
[10] *Chung-Ang University, Seoul, 06974, Republic of Korea*
[11] *COMSATS University Islamabad, Lahore Campus, Defence Road, Off Raiwind Road, 54000 Lahore, Pakistan*
[12] *Fudan University, Shanghai 200433, People's Republic of China*
[13] *GSI Helmholtzcentre for Heavy Ion Research GmbH, D-64291 Darmstadt, Germany*
[14] *Guangxi Normal University, Guilin 541004, People's Republic of China*
[15] *Guangxi University, Nanning 530004, People's Republic of China*
[16] *Hangzhou Normal University, Hangzhou 310036, People's Republic of China*
[17] *Hebei University, Baoding 071002, People's Republic of China*
[18] *Helmholtz Institute Mainz, Staudinger Weg 18, D-55099 Mainz, Germany*
[19] *Henan Normal University, Xinxiang 453007, People's Republic of China*
[20] *Henan University, Kaifeng 475004, People's Republic of China*
[21] *Henan University of Science and Technology, Luoyang 471003, People's Republic of China*
[22] *Henan University of Technology, Zhengzhou 450001, People's Republic of China*
[23] *Huangshan College, Huangshan 245000, People's Republic of China*
[24] *Hunan Normal University, Changsha 410081, People's Republic of China*
[25] *Hunan University, Changsha 410082, People's Republic of China*
[26] *Indian Institute of Technology Madras, Chennai 600036, India*
[27] *Indiana University, Bloomington, Indiana 47405, U.S.A.*
[28] *INFN Laboratori Nazionali di Frascati, (A)INFN Laboratori Nazionali di Frascati, I-00044, Frascati, Italy; (B)INFN Sezione di Perugia, I-06100, Perugia, Italy; (C)University of Perugia, I-06100, Perugia, Italy*
[29] *INFN Sezione di Ferrara, (A)INFN Sezione di Ferrara, I-44122, Ferrara, Italy; (B)University of Ferrara, I-44122, Ferrara, Italy*
[30] *Inner Mongolia University, Hohhot 010021, People's Republic of China*
[31] *Institute of Modern Physics, Lanzhou 730000, People's Republic of China*
[32] *Institute of Physics and Technology, Peace Avenue 54B, Ulaanbaatar 13330, Mongolia*
[33] *Instituto de Alta Investigación, Universidad de Tarapacá, Casilla 7D, Arica 1000000, Chile*
[34] *Jilin University, Changchun 130012, People's Republic of China*
[35] *Johannes Gutenberg University of Mainz, Johann-Joachim-Becher-Weg 45, D-55099 Mainz, Germany*
[36] *Joint Institute for Nuclear Research, 141980 Dubna, Moscow region, Russia*
[37] *Justus-Liebig-Universitaet Giessen, II. Physikalisches Institut, Heinrich-Buff-Ring 16, D-35392 Giessen, Germany*
[38] *Lanzhou University, Lanzhou 730000, People's Republic of China*

JHEP11(2024)062

[39] Liaoning Normal University, Dalian 116029, People's Republic of China
[40] Liaoning University, Shenyang 110036, People's Republic of China
[41] Nanjing Normal University, Nanjing 210023, People's Republic of China
[42] Nanjing University, Nanjing 210093, People's Republic of China
[43] Nankai University, Tianjin 300071, People's Republic of China
[44] National Centre for Nuclear Research, Warsaw 02-093, Poland
[45] North China Electric Power University, Beijing 102206, People's Republic of China
[46] Peking University, Beijing 100871, People's Republic of China
[47] Qufu Normal University, Qufu 273165, People's Republic of China
[48] Renmin University of China, Beijing 100872, People's Republic of China
[49] Shandong Normal University, Jinan 250014, People's Republic of China
[50] Shandong University, Jinan 250100, People's Republic of China
[51] Shanghai Jiao Tong University, Shanghai 200240, People's Republic of China
[52] Shanxi Normal University, Linfen 041004, People's Republic of China
[53] Shanxi University, Taiyuan 030006, People's Republic of China
[54] Sichuan University, Chengdu 610064, People's Republic of China
[55] Soochow University, Suzhou 215006, People's Republic of China
[56] South China Normal University, Guangzhou 510006, People's Republic of China
[57] Southeast University, Nanjing 211100, People's Republic of China
[58] State Key Laboratory of Particle Detection and Electronics, Beijing 100049, Hefei 230026, People's Republic of China
[59] Sun Yat-Sen University, Guangzhou 510275, People's Republic of China
[60] Suranaree University of Technology, University Avenue 111, Nakhon Ratchasima 30000, Thailand
[61] Tsinghua University, Beijing 100084, People's Republic of China
[62] Turkish Accelerator Center Particle Factory Group, (A)Istinye University, 34010, Istanbul, Turkey; (B)Near East University, Nicosia, North Cyprus, 99138, Mersin 10, Turkey
[63] University of Bristol, (A)H H Wills Physics Laboratory; (B)Tyndall Avenue; (C)Bristol; (D)BS8 1TL
[64] University of Chinese Academy of Sciences, Beijing 100049, People's Republic of China
[65] University of Groningen, NL-9747 AA Groningen, The Netherlands
[66] University of Hawaii, Honolulu, Hawaii 96822, U.S.A.
[67] University of Jinan, Jinan 250022, People's Republic of China
[68] University of Manchester, Oxford Road, Manchester, M13 9PL, United Kingdom
[69] University of Muenster, Wilhelm-Klemm-Strasse 9, 48149 Muenster, Germany
[70] University of Oxford, Keble Road, Oxford OX13RH, United Kingdom
[71] University of Science and Technology Liaoning, Anshan 114051, People's Republic of China
[72] University of Science and Technology of China, Hefei 230026, People's Republic of China
[73] University of South China, Hengyang 421001, People's Republic of China
[74] University of the Punjab, Lahore-54590, Pakistan
[75] University of Turin and INFN, (A)University of Turin, I-10125, Turin, Italy; (B)University of Eastern Piedmont, I-15121, Alessandria, Italy; (C)INFN, I-10125, Turin, Italy
[76] Uppsala University, Box 516, SE-75120 Uppsala, Sweden
[77] Wuhan University, Wuhan 430072, People's Republic of China
[78] Yantai University, Yantai 264005, People's Republic of China
[79] Yunnan University, Kunming 650500, People's Republic of China
[80] Zhejiang University, Hangzhou 310027, People's Republic of China
[81] Zhengzhou University, Zhengzhou 450001, People's Republic of China

[a] Deceased
[b] Also at the Moscow Institute of Physics and Technology, Moscow 141700, Russia
[c] Also at the Novosibirsk State University, Novosibirsk, 630090, Russia
[d] Also at the NRC "Kurchatov Institute", PNPI, 188300, Gatchina, Russia
[e] Also at Goethe University Frankfurt, 60323 Frankfurt am Main, Germany
[f] Also at Key Laboratory for Particle Physics, Astrophysics and Cosmology, Ministry of Education; Shanghai Key Laboratory for Particle Physics and Cosmology; Institute of Nuclear and Particle Physics, Shanghai 200240, People's Republic of China

JHEP11(2024)062

[g] Also at Key Laboratory of Nuclear Physics and Ion-beam Application (MOE) and Institute of Modern Physics, Fudan University, Shanghai 200443, People's Republic of China
[h] Also at State Key Laboratory of Nuclear Physics and Technology, Peking University, Beijing 100871, People's Republic of China
[i] Also at School of Physics and Electronics, Hunan University, Changsha 410082, China
[j] Also at Guangdong Provincial Key Laboratory of Nuclear Science, Institute of Quantum Matter, South China Normal University, Guangzhou 510006, China
[k] Also at MOE Frontiers Science Center for Rare Isotopes, Lanzhou University, Lanzhou 730000, People's Republic of China
[l] Also at Lanzhou Center for Theoretical Physics, Key Laboratory of Theoretical Physics of Gansu Province, and Key Laboratory for Quantum Theory and Applications of MoE, Lanzhou University, Lanzhou 730000, People's Republic of China
[m] Also at the Department of Mathematical Sciences, IBA, Karachi 75270, Pakistan
[n] Also at Ecole Polytechnique Federale de Lausanne (EPFL), CH-1015 Lausanne, Switzerland
[o] Also at Helmholtz Institute Mainz, Staudinger Weg 18, D-55099 Mainz, Germany

JHEP11(2024)062